

Jørgen Lauritzen Jensen

Quasi-non-linear fracture mechanics analysis of splitting failure in simply supported beams loaded perpendicular to grain by dowel joints

Received: October 18, 2004 / Accepted: January 5, 2005

Abstract A quasi-non-linear fracture mechanics model based on beam on elastic foundation theory is applied for analysis of the splitting failure of dowel joints loaded perpendicular to grain. Simply supported beams symmetrically loaded by two dowels are considered, and the effects of edge distance, dowel spacing, and distance between dowels and supports are accounted for. The foundation modulus used in the beam on elastic foundation model is chosen so that the perpendicular-to-grain tensile strength and fracture energy properties of the wood are correctly represented. This ensures that a conventional stress analysis and failure criterion lead to the same solution as the compliance method of fracture mechanics. A semiempirical efficiency factor is proposed to account for the influence of the total beam depth, which does not enter the beam on elastic foundation model, but the effect of which is evident from tests. It is shown that the so-called Van der Put/Leijten model, which recently has been adopted in Eurocode 5, appears as a special case of the model presented. Tests on simply supported beams with a single dowel joint at midspan are compared with the theoretical predictions. Various edge distances, beam depths, and spans were tested.

Key words Dowel joints · Perpendicular to grain · Splitting · Fracture mechanics · Beam on elastic foundation

Introduction

A dowel-type fastener joint loading a beam perpendicular to grain may fail in a ductile manner, characterized by bend-

ing of the fasteners and/or embedment of the fasteners into the wood, or it may cause a brittle failure in the beam characterized by splitting of the wood. The ductile failure modes are well understood and can be predicted fairly accurately by the European Yield Model,¹ which now forms the basis of design of dowel-type fastener joints in major design codes. Only recently, a number of simple analytical models based on fracture mechanics have been proposed^{2–7} for prediction of brittle failure, but none has yet gained wide acceptance.

A quasi-non-linear fracture mechanics model based on beam on elastic foundation (BEF) theory was previously presented.⁶ The model presented in this article is based on the same ideas, but is extended to take into account the influence of the supports in simply supported beams.

Application of the BEF theory can only be expected to lead to reasonable results for edge distances, h_e , which are relatively small compared with the total beam depth, h . By nature, the BEF model does not predict any influence of h . However, tests clearly indicate the counterintuitive effect that the failure load increases if h decreases for constant h_e . In the present article a semiempirical approach is suggested for modifying the model to produce reasonable solutions for larger h_e/h ratios (a). The suggested modification makes the presented model contain previous models^{2,5} as special cases.

Theory

A structure as shown in Fig. 1 is considered. The part of the beam below the dowels in Fig. 1 is supposed to behave as a beam (beam depth: h_e) on an elastic foundation. The part of the beam above the dowels is supposed to provide the foundation.

The symmetrical half of the structure is modeled as shown in Fig. 2. Note that the structure analyzed previously⁶ (hereafter denoted as “plate joint”) differs from Fig. 2 by having no point support at the right end.

J.L. Jensen (✉)
Institute of Wood Technology, Akita Prefectural University,
11-1 Kaiezaka, Noshiro 016-0876, Japan
Tel. +81-185-52-6985; Fax +81-185-52-6976
e-mail: jensen@iwt.akita-pu.ac.jp

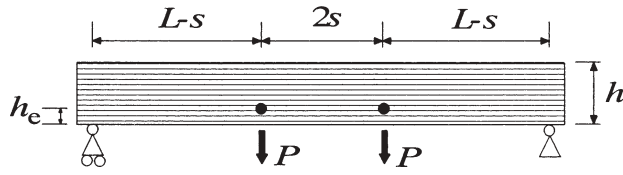


Fig. 1. Geometry of structure

The foundation stress, $\sigma(s)$ (tensile stresses are positive), at the location of the dowel is given by

$$\sigma(s) = -Kw(s) \quad (1)$$

where K (unit: N/m^3) is the foundation modulus and $w(s)$ is the deflection of the beam axis.⁸

Failure is assumed to occur when the stress, $\sigma(s)$, equals the tensile strength perpendicular to grain, f_t , of the wood, leading to the failure load, P_c .

The foundation is intended to model the strength and fracture performance of the wood perpendicular to grain. The damage and fracture performance of wood is non-linear, but is in the present analysis represented by a linear response that is equivalent in terms of peak stress, f_t , and fracture energy dissipation, G_f . Because the energy dissipation in the case of linear performance is

$$G_f = \frac{1}{2} f_t \left(\frac{f_t}{K} \right) \quad \text{it follows that} \quad K = \frac{f_t^2}{G_f} \quad (2)$$

The solution to the governing differential equations for a Timoshenko beam on elastic foundation falls into two cases, the limit between which may be characterized by a requirement to the depth, h_e , of the beam on elastic foundation (rectangular cross section)

$$\text{Case 1: } h_e \leq \frac{200}{3} \frac{G^2}{E} \frac{G_f}{f_t^2} \quad \text{Case 2: } h_e \geq \frac{200}{3} \frac{G^2}{E} \frac{G_f}{f_t^2} \quad (3)$$

where E is the modulus of elasticity in the grain direction and G is the shear modulus.

For the beam shown in Fig. 2, the failure load is found to be

Case 1:

$$P_c = \frac{8bf_t u_1 v_1}{u_1(3v_1^2 - u_1^2)\chi_1 - v_1(3u_1^2 - v_1^2)\chi_2}$$

$$\chi_1 = \frac{\sinh 2v_1 L + \sinh 2v_1(L-s)\cos 2u_1 s - \cos 2u_1(L-s)\sinh 2v_1 s}{\sinh^2 v_1 L + \cos^2 u_1 L}$$

$$\chi_2 = \frac{\sin 2u_1 L + \sin 2u_1(L-s)\cosh 2v_1 s - \cosh 2v_1(L-s)\sin 2u_1 s}{\sinh^2 v_1 L + \cos^2 u_1 L}$$

$$u_1^2 = \frac{1}{2}\sqrt{\lambda} - \frac{1}{4}\eta, \quad v_1^2 = \frac{1}{2}\sqrt{\lambda} + \frac{1}{4}\eta$$

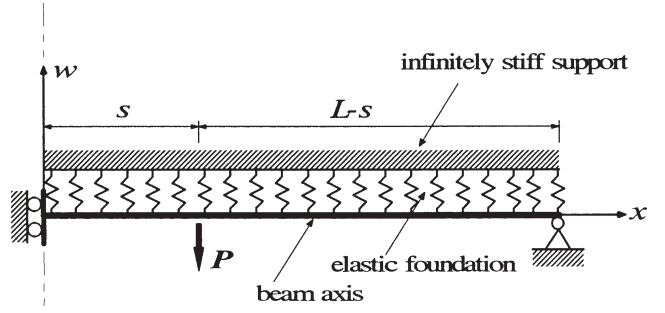


Fig. 2. Beam on elastic foundation model

Case 2:

$$P_c = bf_t \frac{v_2^2 - u_2^2}{v_2^3 \frac{\sinh v_2(L-s)}{\cosh v_2 L} \cosh v_2 s - u_2^3 \frac{\sinh u_2(L-s)}{\cosh u_2 L} \cosh u_2 s}$$

$$u_2^2 = \frac{1}{2}\eta - \sqrt{\frac{1}{4}\eta^2 - \lambda}, \quad v_2^2 = \frac{1}{2}\eta + \sqrt{\frac{1}{4}\eta^2 - \lambda} \quad (4b)$$

where

$$\lambda = \frac{Kb}{EI}, \quad \eta = \frac{Kb}{GA_s} \quad (5)$$

b being the width of the beam, I the moment of inertia, and A_s is the equivalent shear area of the beam cross section ($A_s = 5bh_e/6$ and $I = bh_e^3/12$ for a rectangular cross section with beam depth h_e).

Infinitely long beam with two dowels

For an infinitely long beam ($L \rightarrow \infty$), the failure load is reduced to (for u_1 , u_2 , v_1 , and v_2 , see Eq. 4)

Case 1:

$$P_c = \frac{4bf_t u_1 v_1}{u_1(3v_1^2 - u_1^2)(1 + e^{-2v_1 s} \cos 2u_1 s) + v_1(3u_1^2 - v_1^2)e^{-2v_1 s} \sin 2u_1 s} \quad (6a)$$

$$\text{Case 2: } P_c = 2bf_t \frac{v_2^2 - u_2^2}{v_2^3(1 + e^{-2v_2 s}) - u_2^3(1 + e^{-2u_2 s})} \quad (6b)$$

which is the same solution as previously obtained.⁶

(4a)

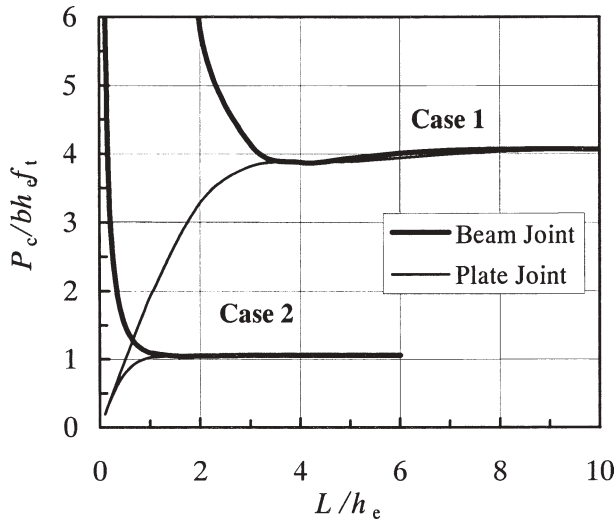


Fig. 3. Plate joint and beam joint solutions

Finite beam with one dowel

The failure load, P_c , for a beam with a single dowel is obtained from Eq. 4 by setting $s = 0$ (and multiplying by 2). For u and v , see Eq. 4.

$$\text{Case 1: } P_c = 8bf_t \frac{\sinh^2 v_1 L + \cos^2 u_1 L}{\frac{3v_1^2 - u_1^2}{v_1} \sinh 2v_1 L - \frac{3u_1^2 - v_1^2}{u_1} \sin 2u_1 L} \quad (7a)$$

$$\text{Case 2: } P_c = 2bf_t \frac{v_2^2 - u_2^2}{v_2^3 \tanh v_2 L - u_2^3 \tanh u_2 L} \quad (7b)$$

Infinitely long beam with one dowel

For an infinitely long beam with a single dowel, the previously obtained solution⁶ is arrived at

$$P_c = \gamma P_{c,\text{LEFM}} \quad (8)$$

where the linear elastic fracture mechanics solution, $P_{c,\text{LEFM}}$, is given by

$$P_{c,\text{LEFM}} = 2bC_1 \sqrt{h_c}, \quad C_1 = \sqrt{\frac{5}{3} G G_f} \quad (9)$$

and γ is given by

$$\gamma = \frac{\sqrt{2\xi + 1}}{\xi + 1}, \quad \xi = \frac{C_1}{f_t} \sqrt{10 \frac{G}{E} \frac{1}{h_c}} \quad (10)$$

The above failure loads were derived using a conventional stress analysis and failure criterion, and fracture mechanics enters the model through the constitutive relation adopted for the foundation. This analysis is an exact analogy to the quasi-non-linear analysis of lap joints.⁹

It has previously been demonstrated that the linearized constitutive assumption (Eq. 2) used in the BEF model makes the stress approach lead to the same solution obtained by the compliance method.^{10,11}

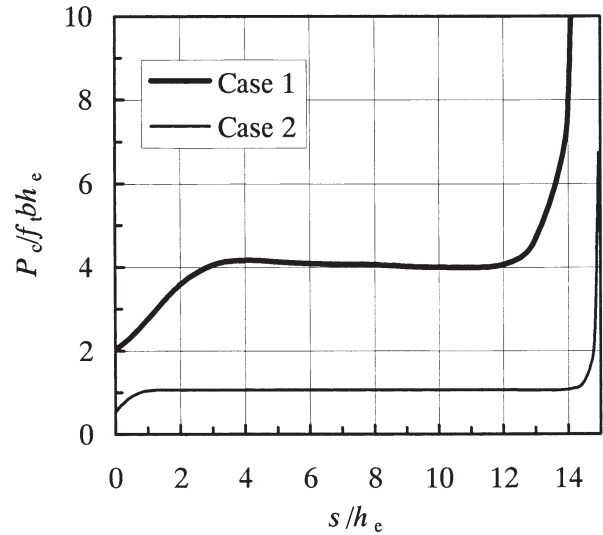


Fig. 4. Effect of dowel spacing and supports

Figure 3 shows the investigation of a specimen with a single dowel (or joint) at midspan. The beam joint solution (Eq. 7) is compared with the plate joint solution⁶ (i.e., no point support at the right end in Fig. 2). Examples showing case 1 and case 2 solutions are given. In both examples, $E = 12700 \text{ MPa}$, $G = 870 \text{ MPa}$, and edge distance $h_e = 56 \text{ mm}$. For case 1, the fracture properties reported for laminated veneer lumber (LVL),⁵ $f_t = 0.89 \text{ MPa}$, $G_f = 0.25 \text{ N/mm}$ are used. For case 2, $f_t = 5.0 \text{ MPa}$ and $G_f = 0.30 \text{ N/mm}$.

In Fig. 4, a simply supported beam with two dowels (or joints) is examined. The effect of dowel spacing, $2s$, and the influence of supports according to Eq. 4 is shown for a beam of length $L = 15h_e$ ($h_e = 56 \text{ mm}$) using the same material properties as in Fig. 3.

Modification of foundation stiffness

In the BEF theory described above, the foundation is assigned the stiffness as given by Eq. 2. This may be a good approximation for small values of $\alpha = h_c/h$, but for large values of α the completely stiff support of the springs as shown in Fig. 2 is not a realistic assumption.

K_s denotes an additional contribution to the foundation stiffness due to the deflection of the part of the beam above the potential crack path (beam depth: $(1 - \alpha)h$). It is here assumed that K_s can be written as

$$K_s = K \left(\frac{1 - \alpha}{\alpha} \right)^m \quad (11)$$

where $\alpha = h_c/h$, K is given by Eq. 2, and m is a parameter to be determined empirically. Note that $m = 1$ corresponds to $K_s/K = A_{s1}/A_{s2}$, and $m = 3$ corresponds to $K_s/K = EI_1/EI_2$, where subscript 1 refers to the beam part above the potential crack path (foundation) and subscript 2 refers to the beam part below the potential crack path (beam on elastic foundation).

The modified foundation stiffness is given by

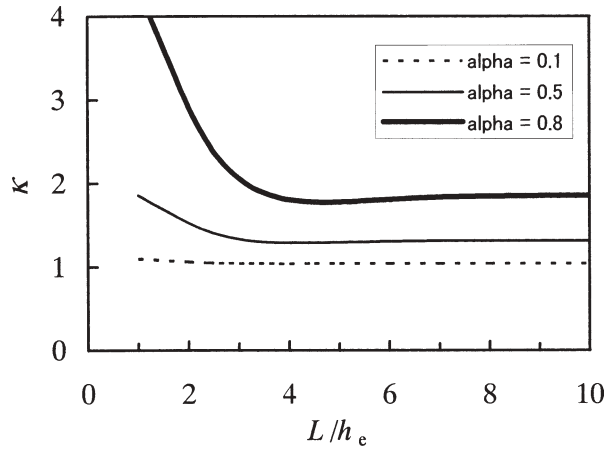


Fig. 5. Effect of modification of foundation stiffness

$$K_{\text{mod}} = \frac{KK_s}{K + K_s} = \varphi K, \quad \varphi = \frac{1}{1 + \left(\frac{\alpha}{1 - \alpha}\right)^m} \quad (12)$$

or, by use of Eq. 2

$$K_{\text{mod}} = \frac{f_t^2}{2G_{f,\text{mod}}}, \quad G_{f,\text{mod}} = \frac{1}{\varphi} G_f \quad (13)$$

Setting $m = 1$ results in $\varphi = 1 - \alpha$, i.e.,

$$G_{f,\text{mod}} = \frac{1}{1 - \alpha} G_f \quad (14)$$

The additional foundation stiffness as introduced by Eq. 11 is constant along the beam axis, whereas a proper account for the additional deflections of the part of the beam above the crack (beam depth: $(1 - \alpha)h$) would involve a foundation stiffness that varies along the beam axis. The modification of the foundation stiffness as suggested here may therefore be considered a semiempirical attempt to involve the influence of the total beam depth, h .

Figure 5 shows an example of the influence of the modified foundation stiffness as given by Eq. 14. A simply supported beam with a single joint at midspan ($b = 25$ mm, $h_e = 40$ mm, $E = 7880$ MPa, $G = 438$ MPa, $f_t = 1.2$ MPa, and $G_f = 0.16$ N/mm) was analyzed by means of Eq. 7. The efficiency factor, κ , is defined as $\kappa = P_c(K_{\text{mod}})/P_c(K)$, where $P_c(K_{\text{mod}})$ is the failure load obtained using K_{mod} and $P_c(K)$ is the failure load using K .

Figure 5 shows that the efficiency factor depends not only on the α value (h_e/h), but also on the L/h_e ratio. For $L/h_e \rightarrow \infty$, κ asymptotically approaches κ_∞ .

$$\kappa_\infty = \rho \frac{\zeta + 1}{\sqrt{2\zeta + 1}} \frac{\sqrt{2\rho\zeta + 1}}{\rho\zeta + 1}$$

$$\rho = \frac{1}{\sqrt{1 - \frac{h_e}{h}}}, \quad \zeta = \frac{C_1}{f_t} \sqrt{10 \frac{G}{E} \frac{1}{h_e}}, \quad C_1 = \sqrt{\frac{5}{3} G G_f} \quad (16)$$

Instead of using the modified value of the fracture energy as given by Eq. 14, the modification factor, κ_∞ , as given by Eq. 16, may be used as a semiempirical efficiency factor, by which the solutions given by Eqs. 4, 6, 7, and 8 may be

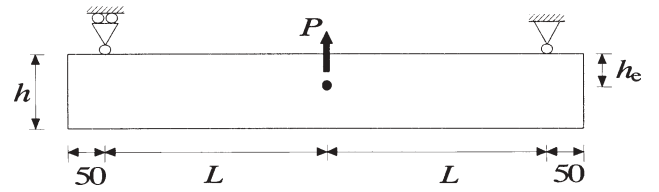


Fig. 6. Test setup

multiplied to account for the effect of the total beam depth, h . Although theoretically not strictly conservative for all L/h_e values (e.g., according to Fig. 5, κ assumes a minimum value for L/h_e values between 4 and 6 for $\alpha = 0.8$), κ_∞ seems to be a practical and safe simplification.

It is noted that $\kappa_\infty \rightarrow \rho$ for $f_t \rightarrow \infty$. The Van der Put/Leijten solution^{2,7} is thus obtained by multiplying Eq. 8 by κ_∞ and assuming $f_t \rightarrow \infty$. The Van der Put/Leijten solution seems to give a prediction of the influence of the total beam depth, h , in good agreement with test results.²⁻⁴ It is further noted that $\kappa_\infty \rightarrow 1$ for $\alpha = h_e/h \rightarrow 0$. The Gustafsson/Larsen model⁵ is thus obtained by assuming $\alpha \rightarrow 0$ and $f_t \rightarrow \infty$.

Experimental

Materials and methods

Simply supported glulam beams of Japanese cedar (*Cryptomeria japonica*) were tested using joints with a single dowel as shown in Fig. 6.

The glulam was made of 30-mm laminae of the same grade (machine graded). Specimens were cut from eight beams (100×200 mm² cross section) of which the modulus of elasticity (MOE) was measured (longitudinal vibration frequency). MOE ranged from 7500 MPa to 8250 MPa (mean value: 7880 MPa). Moisture content (MC) was 12.5%. Density ranged from 362 kg/m³ to 392 kg/m³ (mean value: 373 kg/m³) at the given MC. Only knot-free specimens were used in order to limit the variation. In all cases beam width was $b = 25$ mm, and a 14-mm dowel was used in a 15-mm hole. The load was displacement controlled, and time to failure was 2–3 min.

Two different edge distances, $h_e = 20$ mm and $h_e = 40$ mm, were tested. Edge distance $h_e = 20$ mm was tested for $h = 200$ mm and $h = 100$ mm (i.e., $\alpha = h_e/h = 0.1$ and 0.2). For each beam depth $L/h_e = 2.5, 5, 7.5,$ and 10 were tested. Edge distance $h_e = 40$ mm was tested for $h = 200$ mm and $h = 80$ mm (i.e., $\alpha = h_e/h = 0.2$ and 0.5). For $h = 200$ mm, $L/h_e = 2.5, 5,$ and 23.75 were tested. For $h = 80$ mm, $L/h_e = 2.5, 5,$ and 7.5 were tested. Nine to 12 specimens were tested for each condition.

Tests were also conducted on double cantilever beam (DCB) specimens and on so-called plate-joint specimens, as shown in Fig. 7. All specimens were selected to avoid knots. The DCB specimens were used to determine the fracture energy. Thirteen specimens were tested, $b = 25$ mm, $h = 40$ mm, $L = 500$ mm, $a = 200$ mm.

The plate joint specimens were tested for comparison with the beam tests ($b = 25$ mm, $h = 200$ mm, $L = 550$ mm). Eight specimens were tested for $h_e = 20$ mm and $h_e = 40$ mm.

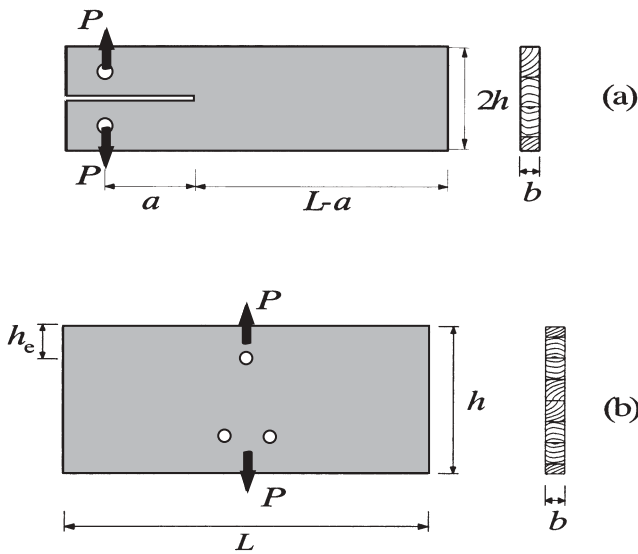


Fig. 7. Geometry of double cantilever beam (a) and plate joint (b) specimens

Results and discussion

Failure load

Fracture energy was determined from the DCB test results using Eq. 17,⁵ resulting in $G_f = 0.16 \pm 0.05 \text{ N/mm}$.

$$G_f = 12 \frac{P_c^2}{b^2 h^3 E} (a + \Delta a)^2, \quad \Delta a = h \sqrt{\frac{E}{10G}} \quad (17)$$

The plate joint tests resulted in: $P_c = 2054 \pm 336 \text{ N}$ for $h_c = 20 \text{ mm}$, and $P_c = 2867 \pm 371 \text{ N}$ for $h_c = 40 \text{ mm}$.

The results of the beam tests are shown in Fig. 8 along with the theoretical predictions given by Eq. 7b and multiplied by the modification factor, κ_z , given by Eq. 16. The following material properties were used: $E = 7880 \text{ MPa}$ and $G_f = 0.16 \text{ N/mm}$ as determined by testing, $G = E/18 = 438 \text{ MPa}$, and $f_t = 1.2 \text{ MPa}$. The perpendicular-to-grain tensile strength is highly volume dependant, and direct determination by testing is questionable because an appropriate size and shape of the test specimen is not obvious. f_t has therefore not been determined by testing, but used as a (constant) “fitting” parameter. Using $f_t = 1.2 \text{ MPa}$, the above given failure loads of the plate joint tests lead to $P_c/bh_c f_t = 3.42$ for $h_c = 20 \text{ mm}$, and $P_c/bh_c f_t = 2.39$ for $h_c = 40 \text{ mm}$. These values are also indicated in Figs. 8–11, and as expected, the failure loads of the plate joints are very close to those of the long beams for small values of a , while the plate joints give conservative results for large values of a . As shown in Fig. 6, a constant overhang (distance from support to beam end) of 50 mm was used in the beam tests. For small values of L/h_c , however, it was suspected that the overhang had a significant influence on the failure load (especially for small a values). Supplementary tests were therefore conducted on beams with $h = 200 \text{ mm}$ and $L/h_c = 2.5$ for both $h_c = 20 \text{ mm}$ and $h_c = 40 \text{ mm}$, using an overhang of just 10 mm. The test results are shown in Fig. 8a,c, which shows the significant influence of the overhang.

Failure mechanism

A majority of the long beams ($L/h_c = 5$) failed suddenly without significant stable crack propagation. In a few specimens a crack appeared and propagated at increasing load to a certain critical length, after which sudden failure occurred. The cracks did not extend to the vicinity of the supports.

For short beams ($L/h_c = 2.5$) stable crack growth was observed in all cases. A crack appeared and propagated all the way to the supports at still increasing load. After having reached the supports, the crack seemed to be arrested at (in some cases) still increasing load, after which a sudden decrease in load was observed as the crack propagated past the support to the end of the beam. The failure loads given in Fig. 8 are the maximum loads obtained before this sudden decrease in load. After propagation of the crack to the beam end, the load in some cases increased again to finally end in a bending failure of the beam with depth h_c at a load level slightly higher than shown in the figures; in other cases bending failure occurred when the crack suddenly propagated past the supports to the beam ends. It is obvious that the overhang of 50 mm affects the test results for specimens with $L/h_c = 2.5$. With 10-mm overhang, there was only little increase in load after the crack had reached the supports.

It was expected that the tests would show stronger influence of the supports than predicted by the model, because the model only includes beam actions; arch effects were expected for relatively small L/h_c values. However, the tests, in agreement with the model, show no signs of influence of the supports (when eliminating the effect of overhang) down to $L/h_c = 2.5$.

Tests were also conducted on specimens with $L/h_c = 1.25$. However, these tests were abandoned because excessive embedment occurred without crack propagation. This indicates that the splitting strength, in agreement with the theoretical predictions, increases significantly for L/h_c in the range between 1.25 and 2.5.

Conclusions

A quasi-non-linear fracture mechanics model based on beam on elastic foundation theory was applied to the analysis of splitting failure in simply supported beams with dowel-type fastener connections loaded perpendicular to grain. Tests were conducted on beams with a single dowel at midspan. Of particular interest was the question: how long beams are needed to eliminate the influence of the supports on the failure load?

Tests as well as theoretical predictions show that the supports have no influence for span/edge distance ratios ($2L/h_c$) above 5. The theory predicts that for span/edge distance ratios of less than about 4, the supports have a strong influence on the failure load. For a span/edge distance ratio ($2L/h_c$) of 2.5, tests resulted in constantly increasing embedment without splitting failure.

The tests indicate that the theoretical model agrees very well with experiments not only in terms of the influence of

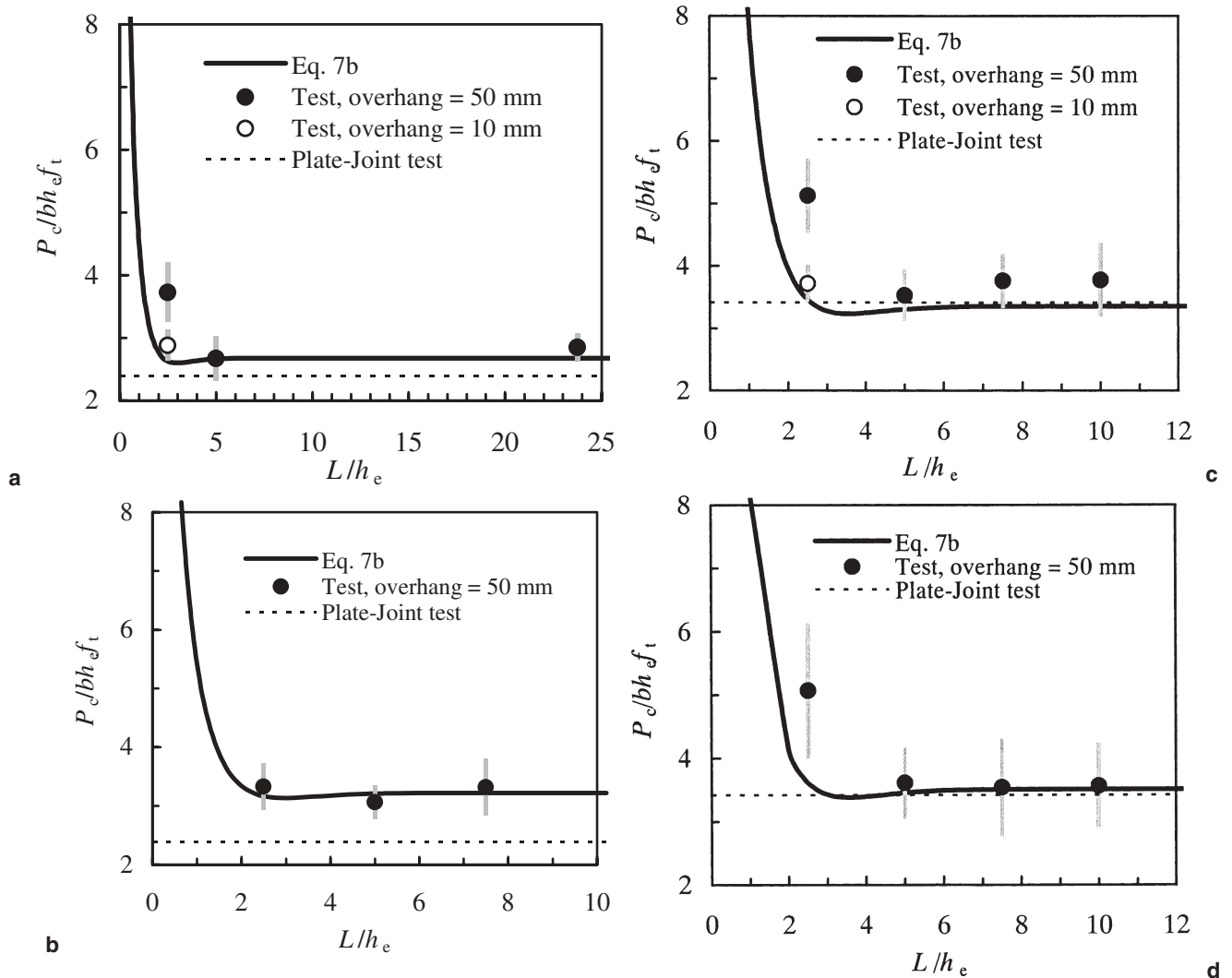


Fig. 8. Failure load as a function of span for **a** $h_e = 40$ mm, $h = 200$ mm; **b** $h_e = 40$ mm, $h = 80$ mm; **c** $h_e = 20$ mm, $h = 200$ mm; **d** $h_e = 20$ mm, $h = 100$ mm. For test results, mean values \pm standard deviations are given

the supports, but also with regard to the influence of edge distance, h_e , and total beam depth, h . The model presented includes important previous models such as the Van der Put/Leijten model² and the Gustafsson/Larsen model⁵ as special cases.

References

- Johansen KW (1941) Forsøg med træforbindelser. Bygningsstatistiske Meddelelser, årgang XII
- Van der Put TACM, Leijten AJM (2000) Evaluation of perpendicular-to-grain failure of beams caused by concentrated loads of joints. In: Proceedings of the International Council for Research and Innovation in Building and Construction, CIB-W18 Meeting Thirty-Three, Delft, The Netherlands, paper No. 33-7-7
- Leijten AJM, Jorissen AJM (2001) Splitting strength of beam loaded by connections perpendicular to grain, model validation. In: Proceedings of the International Council for Research and Innovation in Building and Construction, CIB-W18 Meeting Thirty-Four, Venice, Italy, paper No. 34-7-1
- Leijten AJM (2002) Splitting strength of beams loaded by connections, model comparison. In: Proceedings of the International Council for Research and Innovation in Building and Construction, CIB-W18 Meeting Thirty-Five, Kyoto, Japan, paper No. 35-7-7
- Gustafsson PJ, Larsen HJ (2001) Dowel joints loaded perpendicular to grain. In: Aicher S, Reinhardt HW (eds) Joints in timber structures. Proceedings of the International RILEM Symposium, Stuttgart, Germany, pp 577–586
- Jensen JL, Gustafsson PJ, Larsen HJ (2003) A tensile fracture model for joints with rods or dowels loaded perpendicular to grain. In: Proceedings of the International Council for Research and Innovation in Building and Construction, CIB-W18 Meeting Thirty-Six, Colorado, USA, paper No. 36-7-9
- Jensen JL (2003) Splitting strength of beams loaded by connections. In: Proceedings of the International Council for Research and Innovation in Building and Construction, CIB-W18 Meeting Thirty-Six, Colorado, USA, paper No. 36-7-8
- Pilkey WD (1994) Formulas for stress, strain, and structural matrices. Wiley, New York
- Gustafsson PJ (1987) Analysis of generalized Volkersen-joints in terms of non-linear fracture mechanics. In: Verchery G, Cardon AH (eds) Mechanical behaviour of adhesive joints. Pluralis, Paris, pp 323–338
- Jensen JL (2005) Quasi-non-linear fracture mechanics analysis of the double-cantilever-beam specimen. *J Wood Sci* 51:566–571
- Jensen JL (2005) Quasi-non-linear fracture mechanics analysis of the splitting failure of single dowel joints loaded perpendicular to grain. *J Wood Sci* 51:559–565